Case Studies in Thermal Engineering 23 (2021) 100823

Contents lists available at ScienceDirect

Case Studies in Thermal Engineering

journal homepage: http://www.elsevier.com/locate/csite

Upgrading properties of biochar fuel derived from cassava rhizome via torrefaction: Effect of sweeping gas atmospheres and its economic feasibility

Kamonwat Nakason [a,b,*], Pongtanawat Khemthong [c], Wasawat Kraithong [c], Parinvadee Chukaew [a,b], Bunyarit Panyapinyopol [a,b], Duangta Kitkaew [a,b], Prasert Pavasant [d]

[a] Department of Sanitary Engineering, Faculty of Public Health, Mahidol University, Bangkok, Thailand
[b] Center of Excellence on Environmental Health and Toxicology (EHT), Bangkok, Thailand
[c] National Nanotechnology Center (NANOTEC), National Science and Technology Development Agency (NSTDA), Pathumthani, Thailand
[d] Tree Moments Co. Ltd., Bangkok, Thailand

GRAPHICAL ABSTRACT

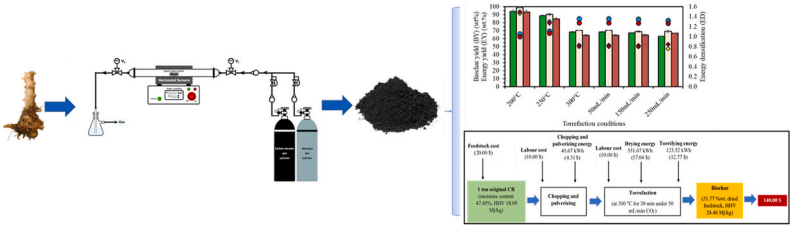

ARTICLE INFO

Keywords:
Torrefaction atmosphere
Biocoal
Torrefaction economic
Agricultural waste
Renewable energy
Torrefaction feasibility

ABSTRACT

Torrefaction is a promising biomass thermal conversion technology to produce biochar due to its ease of operation and mild operating conditions. In this study, cassava rhizome (CR) was torrified under various sweeping gas types (nitrogen (N_2), carbon dioxide (CO_2), mixture gas ($N_2 + CO_2$)) and flow rates (50, 150, 250 mL/min) at 200–300 °C for 30 min. The experimental results show that fuel properties of CR were remarkably upgraded after torrefaction. Sweeping gas has less effect on fuel properties of torrified CR than torrefaction temperature. Torrefaction under CO_2 atmosphere produced the biochar with minimum ash content. Torrefaction at 300 °C under 50 mL/min CO_2 was recommended as the promising condition to produce biochar replacing lignite coal. Thermal properties and chemical functional groups of the derived biochar suggested that

* Corresponding author. Department of Sanitary Engineering, Faculty of Public Health, Mahidol University, Bangkok, Thailand.
E-mail address: kamonwat.nak@mahidol.ac.th (K. Nakason).

https://doi.org/10.1016/j.csite.2020.100823
Received 9 July 2020; Received in revised form 2 December 2020; Accepted 19 December 2020
Available online 23 December 2020

torrefaction process removed mainly oxygen and hydrogen contents which could be achieved through decarbonization (DC), dehydrogenation (DH), and deoxygenation (DO) pathways. Economic feasibility revealed that the torrefaction of CR is cost-advantage under the proposed condition.

1. Introduction

Biomass has been considered as the promising renewable energy alternative. However, the uses of untreated biomass to replace fossil fuels suffer many restrictions such as high humidity and volatile contents, low energy content and density, hydrophilicity, and biodegradation [1]. To overcome these limitations, several technologies have been developed for upgrading biomass to biofuels [2] for example torrefaction, pyrolysis and hydrothermal carbonization. Among these, torrefaction offers several operational advantages due to its ease of operation and mild operating conditions. Torrefaction is a thermal biomass upgrading technology to biochar. This process is normally operated under inert atmospheric at ambient pressure and temperature of 200–300 °C [3]. During a process, both the evaporation of volatile compositions and thermal degradation of lignocellulosic biomass through various reactions, and generate a solid biochar product with a high calorific, hydrophobicity, and grindability properties [4,5]. Hence, torrefaction can help reduce milling, storage, and transportation costs, and improve storage properties of biomass [6–8]. Recently, torrefaction process was examined and tested with several biomass feedstocks such as sugarcane bagasse [9], de-oiled Jatropha seed kernel [8], and cotton stalk [10] with positive results.

Cassava rhizome (CR) is one plentiful agricultural waste biomass in Thailand. In 2019, the amount of cassava product in Thailand reached 31 million tons [11], and this is equivalent to the generation of 6.2 million tons of CR (1 ton of cassava produces 0.2 ton CR) [12]. Generally, CR has been commonly disposed of by open combustion, leading to several severe environmental problems, particularly an increase in fine particulate matter as PM_{10}/$PM_{2.5}$ in the air. To avoid this, there is a need to find viable alternative in order to convert CR to other value-added products including bio-oil [13], acetone-butanol-ethanol [14], hydrochar, and building-block chemicals [15]. However, such alternatives still suffer feasibility problems due to the high biomass treatment costs. In this study, the conversion of CR to biochar as coal replacing material through torrefaction is proposed targeting at the reduced operating costs through the use of alternative sweeping gas. Sweeping gas is one of the vital torrefaction parameters related with an operational expenditure, and in the present work, a cheaper carbon dioxide (CO_2) was used to replace a more costly industrial grade nitrogen (N_2). The use of CO_2 does not only help with the cost-effectiveness of the torrefaction, but also could reduce the greenhouse gas emission as it can be freely obtained as a combustion waste gas. However, the effect of CO_2 sweeping gas on fuel properties of biochar from torrefaction of CR have not previously investigated.

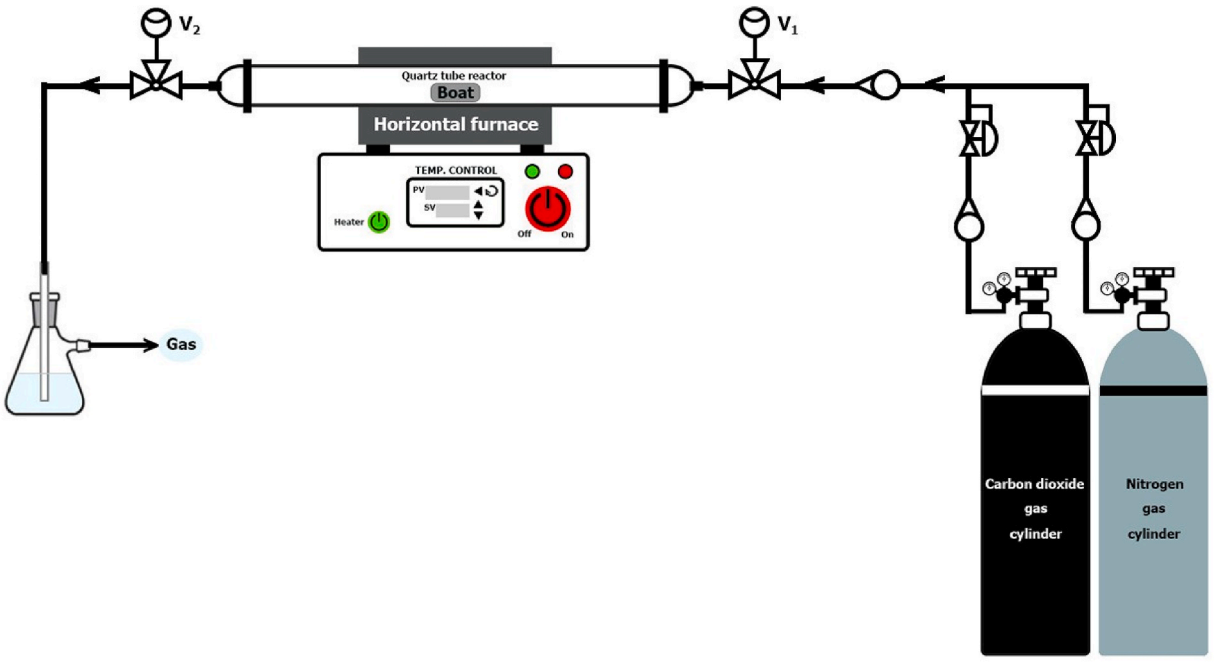

Fig. 1. Instrumental setup for torrefaction process.

2. Materials and methods

2.1. Feedstock preparation

CR containing 47.45% moisture was collected from Dan Makham Tia District, Kanchanaburi Province, Thailand. It was cleaned with tap water to eliminate dust and soil, then chopped to a small piece with size of 3–5 cm. After that, the chopped CR was dried at 70 °C for 24 h, and pulverized to the powder with particle size of 0.3–0.5 mm. The pulverized CR was later dried at 105 °C for 24 h and stored in a sealed plastic bag for further torrefaction process.

2.2. Torrefaction experiment

Torrefaction process were conducted under ambient atmospheric of N_2, CO_2, and mixed N_2: CO_2 gases (ratio 1:1) with flow rates of 50, 150, and 250 mL/min. Various torrefied temperatures were investigated at 200, 250, and 300 °C. The torrefaction instrument is depicted in Fig. 1, consisting N_2 and CO_2 gas cylinders, gas rotameters, quartz tubular reactor (100 cm length, 4.6 cm OD, 4.4 cm ID), quartz boat (10 cm length, 3.6 cm ID, 2.0 cm height), horizontal tube furnace (15 cm heated zone length, 4.6 cm ID), back pressure valve, three way ball valve and gas cleaning unit. Temperature profiles of the horizontal tube furnace (Fig. 2) determined that the times for rising temperature from ambient to target temperatures of 200, 250, and 300 °C are 17, 22, and 27 min, respectively. For each experiment, 3 g of dried CR powder was filled into quartz boat, then placed in the tubular reactor. After that, 250 mL/min of atmospheric gas was flowed through the reactor for 15 min to obtain an innert atmosphere, then the sample was heated to the process temperature with ramping rate of 10 °C/min under desired atmospheric gas. The reaction time was held for 30 min at a desired temperature, then naturally dropped to 90 °C. The biochar was weighed and stored in a sealed plastic bags for further analysis. Each condition was conducted in duplications. If the inconsistent result was appeared, the third was also conducted. The biochar samples were labelled as TTFFG, where TT denotes process temperature, FF denotes gas flow rate, and G denotes atmospheric gas types (N: N_2, C: CO_2, NC: the mixed N_2 and CO_2 gases). For example, the biochar with label of 3005NC referred that the biochar resulted from torrefaction of 300 °C under 50 mL/min mixture gas.

2.3. Product characterization

Biochar from CR torrefaction was characterized in the parameters of mass yield, proximate and ultimate compositions, calorific value, thermal stability characteristics, chemical functional groups, and surface morphology. For proximate compositions, ash and volatile matter (VM) contents were analyzed following the standard analysis methods of NREL/TP-510-42,622 [16] and ASTM D 7582 [17], respectively. Fixed carbon (FC) content was quantified by deducting 100% from moisture, VM, and ash contents. For ultimate compositions, carbon (C), hydrogen (H), nitrogen (N), and sulfur (S) contents were investigated using elemental analyzer (LECO CHNS628, LECO, USA). Oxygen content was defined by deducting 100% from CHNS and ash contents. Calorific value was measured through bomb calorimeter (LECO AC500, LECO, USA). Thermal stability characteristics was investigated using a thermogravimetrical analyzer (TGA/SDTA851e METTLER TOLEDO, USA). Samples were heated from 30 to 850 °C with 10 °C/min ramping rate under 50 mL/min N_2 gas. Chemical functional groups were identified through Fourier Transform Infrared (FTIR) spectroscopy (Thermo Scientific Nicolet 6700, Thermo Scientific, USA) equipped with diamond attenuated total reflectance (ATR). The infrared spectra were scanned from 4000 to 400 cm^{-1} at 64 scans for a resolution of 4 cm^{-1}. The morphology of samples was observed using scanning electron microscopy (SEM, Hitachi S–3400 N, Japan), the samples were coated with goal prior to image.

2.4. Calculation

Biochar yield (BY), fuel ratio, energy densification (ED), energy yield (EY), HHV improvement (HHV_i) are calculated through Eq. (1) – (5):

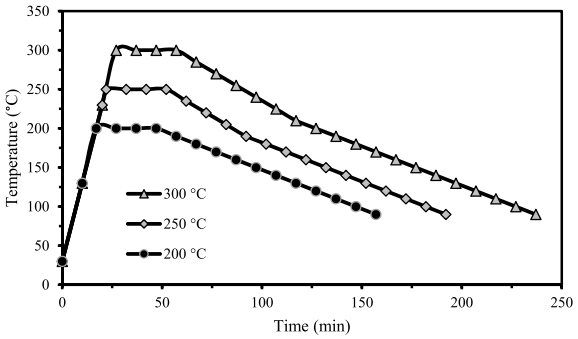

Fig. 2. Temperature profile of horizontal tube furnace.

$$\text{BY (\%)} = \text{(Biochar mass / Dried CR mass) x 100\%} \quad (1)$$

$$\text{Fuel ratio} = \text{FC/VM} \quad (2)$$

$$\text{ED} = \text{Biochar HHV / Dried CR HHV} \quad (3)$$

$$\text{EY (\%)} = \text{BY} \times \text{(Biochar HHV / Dried CR HHV)} \quad (4)$$

$$\text{HHV}_i = \text{(Biochar HHV - Dried CR HHV) / Dried CR HHV} \quad (5)$$

Deoxygenation (DO) is determined using Eqs. (6)–(8) [18]:

$$O_o\ (g) = M_0 \text{ x } (100 - W_0 - A_0) \text{ x } 10^{-2} \text{ x } Y_{o,0} \quad (6)$$

$$R_o\ (g) = M_0 \text{ x SY x } (100 - W_t - A_T) \text{ x } 10^{-2} \text{ x } Y_{o,T} \quad (7)$$

$$\text{DO (\%)} = 1 - (R_o/O_o) \text{ x } 100 \quad (8)$$

where O_o and R_o denote the content of oxygen in dried CR and biochar, respectively. M, W, A, and Y are the sample weight (g), water content (%), ash content (%), and mass fraction of oxygen, respectively. The subscripts 0 and t represent the raw material and torrefaction condition, respectively. Dehydrogenation (DH), and decarbonization (DC) are also determined with the same procedures.

3. Results and discussion

3.1. Biochar yield

Biochar yield (BY) is one of the crucial indexes that can be used to examine the effect of torrefaction on fuel properties of biochar. Fig. 3 shows the effects of process temperatures, atmospheric types, and gas flow rates on BY. It was found that BY values from CR torrefaction under nitrogen (N_2), carbon dioxide (CO_2), and mixture gase ($N_2 + CO_2$) atmosphere continuously decreased from 91.39 to 50.21%, 93.46 to 51.77%, and 93.38 to 50.24% with increasing process temperature, respectively. Decreasing of BY was principally due to the evaporation of volatile compositions [19], decomposition of hemicellulose, and partial decomposition of cellulose and lignin [20]. Interestingly, the BY indexes were independent of sweeping gas type, and gas flow rate, i.e. BY from torrefaction under 50 mL/min CO_2 (51.77%) was only marginally higher than that under either N_2 (50.21%) or mixture gas ($N_2 + CO_2$) (50.24%) atmosphere, and BY from torrefaction under 50 mL/min CO_2 (51.77%) was almost the same as that under 150 mL/min (51.44%), and only slightly lower than that under 250 mL/min CO_2 atmosphere (52.81%). These implied that torrefaction can be conducted to produce biochar regardless of sweeping gas type, and flow rate.

3.2. Physicochemical properties of biochar from torrifaction of CR

Physicochemical properties of biochar from torrefaction of cassava rhizome (CR) at various process temperatures (200, 250, 300 °C), sweeping gas types (nitrogen (N_2), carbon dioxide (CO_2), mixture gas ($N_2 + CO_2$)), and flow rates (50, 150, 250 mL/min) are tabulated with proximate and ultimate compositions, and fuel related indexes in Table 1. The results of proximate compositions demonstrated that ash content in biochar at 200 and 250 °C are lower than that in initial CR (4.96%), while the ash content increased with further increasing in process temperature up to 300 °C. Surprisingly, ash content of biochar from torrefaction under CO_2 atmosphere was lower than that under N_2 or mixture gas atmosphere, and the ash content of biochar from torrefaction under 50 mL/min CO_2 atmosphere was lower than that under 150 or 250 mL/min. This was probably due to CO_2 acted a catalytic role of inorganic composition [21]. These results can be concluded that torrefaction under CO_2 atmosphere enhance fuel property of biochar through ash content diminishing and low CO_2 flow rate was suggested for torrefaction. For VM content, it decreased after torrefaction and continuously decreased with increasing process temperature. On the contrary, VM content of biochar from torrefaction under CO_2

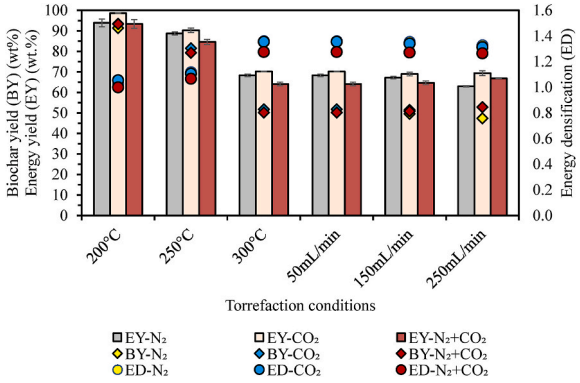

Fig. 3. Yield, energy yield, and energy densification of biochar from torrefaction of CR under different process conditions.

Table 1
Physicochemical properties of CR and biochar from torrifaction of CR at different process conditions.

Sample name	Ultimate analysis (wt.%)					Proximate analysis (wt.%)			Fuel ratio	HHV (Mj/kg)	HHV_i
	C	H	N	S	O	Ash	VM	FC			
CR	45.15	5.83	0.85	0.12	43.09	4.96	77.04	18.00	0.23	18.05	–
Temperature (°C) (Time 30 min, N_2 50 mL/min*)*											
200	46.52	5.72	0.65	0.13	42.22	4.76	73.53	21.71	0.29	18.54	0.03
250	49.92	5.83	0.64	0.12	38.63	4.86	70.06	25.08	0.36	20.18	0.12
300	61.18	4.96	1.11	0.12	23.80	8.83	50.74	40.43	0.80	24.54	0.36
N_2 flow rate (mL/min) (Temperature 300 °C, Time 30 min*)*											
50	61.18	4.96	1.11	0.12	23.80	8.83	50.74	40.43	0.80	24.54	0.36
150	61.26	4.93	1.13	0.13	24.73	7.82	50.41	41.77	0.83	24.45	0.36
250	60.37	4.91	1.12	0.15	26.28	7.17	50.40	42.43	0.84	23.97	0.33
Temperature (°C) (Time 30 min, CO_2 50 mL/min*)*											
200	47.08	6.04	0.47	0.12	42.88	3.40	75.85	20.75	0.27	19.04	0.06
250	49.55	5.80	0.68	0.13	39.23	4.61	71.09	24.30	0.34	19.97	0.11
300	60.94	5.25	0.78	0.12	27.78	5.14	54.27	40.59	0.75	24.46	0.36
CO_2 flow rate (mL/min) (Temperature 300 °C, Time 30 min*)*											
50	60.94	5.25	0.78	0.12	27.78	5.14	54.27	40.59	0.75	24.46	0.36
150	60.30	5.23	0.79	0.11	27.90	5.66	54.35	39.99	0.74	24.20	0.34
250	59.23	5.11	1.01	0.12	27.45	7.08	55.58	37.34	0.67	23.70	0.31
Temperature (°C) (Time 30 min, $N_2 + CO_2$ 50 mL/min*)*											
200	45.37	5.76	0.61	0.17	43.27	4.82	76.01	19.17	0.25	18.04	0.00
250	48.62	5.47	0.69	0.17	38.98	6.08	70.45	23.47	0.33	19.25	0.07
300	58.45	4.83	1.03	0.16	28.02	7.52	52.50	39.99	0.76	23.03	0.28
$N_2 + CO_2$ flow rate (mL/min) (Temperature 300 °C, Time 30 min*)*											
50	58.45	4.83	1.03	0.16	28.02	7.52	52.50	39.99	0.76	23.03	0.28
150	58.45	4.83	0.86	0.12	29.02	6.73	53.68	39.60	0.74	22.94	0.27
250	57.78	4.98	0.76	0.12	29.46	6.91	55.64	37.45	0.67	22.83	0.27

atmosphere was higher than that under N_2 or mixture gas atmosphere, this was probably due to the reactivity of CO_2 was lower than that of N_2 [22]. However, the effect of gas flow rate on VM content was insignificant. Accordingly, FC content in initial CR was enhanced notably after torrefaction and it also continuously enhanced with raising process temperature. Moreover, FC content of biochar from torrefaction under 50 mL/min CO_2 was higher than that under other sweeping gas types. The changes of VM and FC contents were mainly due to devolatilization [22] and thermal cross-link reactions [23]. These results confirmed that 300 °C torrefaction under low CO_2 flow rate (50 mL/min) is the optimal condition for producing solid fuel. Similar result trends of ash, VM, and FC contents were reported in torrefaction of sewage sludge [24], and corncob [5].

For ultimate compositions in Table 1, carbon content of biochar increased substantially, but oxygen and hydrogen contents decreased after torrefaction. Moreover, the carbon content increased continuously with increasing torrefaction temperature while vice versa in oxygen and hydrogen contents. In comparison, sweeping gas types and flow rates affected only marginally to these elemental contents. Increasing carbon as decreasing oxygen and hydrogen contents of biochar was primary due to deoxygenation, dehydrogenation, and decarbonization [18]. Biochar with the promising fuel property need contain high carbon content, thus high torrefaction temperature was suggested as the promising condition for producing biochar as solid fuel from CR.

Fuel related indexes of biochar including fuel ratio, higher heating value (HHV), and higher heating value improvement (HHV_i) are tabulated in Table 1. These indexes significantly correlated with proximate and ultimate compositions. Fuel ratio is determined as the ratio of FC to VM, being used to indicate heating content of solid fuel. In addition, the solid fuel with higher fuel ratio displays a high FC and low VM contents implying the combustion of that solid fuel emitted low volatile gas. Fuel ratio of CR increased substantially after torrefaction and increased continuously with process temperature. However, sweeping gas type, and gas flow rate affected marginally to fuel ratio of biochar. CR biochar with maximum fuel ratio (0.84) could be obtained from torrefaction at 300 °C under 250 mL/min N_2 which was slightly higher than that from torrefaction under 50 mL/min CO_2 (0.75). HHV represents calorific content of solid fuel. CR HHV enhanced after torrefaction and enhanced remarkably at severe torrefaction. Nevertheless, sweeping gas type, and gas flow rate resulted marginally on biochar HHV. CR biochar with maximum HHV (24.54 Mj/kg) could be obtained from torrefaction at 300 °C under 50 mL/min N_2 which was slightly higher than that from torrefaction under 50 mL/min CO_2 (24.46 Mj/kg). The trends of fuel ratio and HHV in CR biochar was similar to those of corncob biochar [5]. HHV_i is ascribed as the ratio of enhancing HHV to raw material HHV [25]. HHV_i of biochar increased remarkably with torrefaction temperature but it slightly changed with sweeping gas type, and gas flow rate. CR biochar with maximum HHV_i (0.36) could be obtained from torrefaction at 300 °C under 50 mL/min CO_2 or N_2. Fuel ratio, HHV, and HHV_i index implied that torrefaction at high process temperature could be conducted to produce the promising biochar as solid fuel, and the results here also indicated that this could be achieved regardless of sweeping gas type, and gas flow rate.

ED and EY of biochar from torrefaction of CR at 200–300 °C under different sweeping gas types (N_2, CO_2, and $N_2 + CO_2$) and flow rates (50, 150, 250 mL/min) is illustrated in Fig. 1. ED determines the densification of energy content in biochar [26]. ED of CR biochar increased noticeably with torrefaction temperature while sweeping gas type and flow rate resulted marginally in ED of CR biochar. The CR biochar with maximum ED (1.36) could be received from torrefaction at 300 °C under 50 mL/min CO_2. EY determines the content of energy in the feedstock contains in the produced biochar from torrefaction [27], this was found to decrease significantly from 98.61

to 70.19% with increasing torrefaction temperature from 200 to 300 °C. In comparison, sweeping gas type and flow rate affected slightly on EY. Interestingly, EY of CR biochar from aggressive torrefaction under CO_2 atmosphere (70.19%) was slightly higher than that under N_2 atmosphere (68.30%). Furthermore, EY of CR biochar from torrefaction under 50 mL/min CO_2 was higher than those under 150 and 250 mL/min CO_2. This phenomenon was associated to BY from CR torrefaction under CO_2 atmosphere (51.77%) was higher than that under N_2 atmosphere (50.24%). In addition, the components of CR biochar could also result EY biochar. CR biochar from torrefaction under CO_2 atmosphere had lower ash content than that under N_2 atmosphere, this resulted in biochar HHV from torrefaction under CO_2 or N_2 atmosphere was quite similar. These results indicated that biochar with the promising fuel property could be produced from torrefaction under low CO_2 flow rate which could reduce the operational expenditure of torrefaction process.

The Van-Krevelen diagram is a valuable graph to interpret the fuel property of solid fuel through the H/C and O/C atomic ratios. For the promising solid fuel, atomic ratios are placed closer to the starting point [28]. The H/C and O/C atomic ratios of initial CR and CR biochar are depicted in Fig. 4, it changed dramatically with torrefaction temperature. An increase in process temperature from 200 to 300 °C during torrefaction under CO_2 atmosphere resulted in H/C and O/C atomic ratios of biochar decreased from 1.54 to 1.03 and 0.68 to 0.34, respectively. This was mainly due to the deoxygenation and decarboxylation reactions. On the other hand, the effect of sweeping gas type and gas flow rate on H/C and O/C atomic ratios were negligible. The figure also provides the atomic ratios of lignite [29], sub-bituminous, and bituminous coal [30], H/C and O/C atomic ratios of CR biochar from 300 °C torrefaction was in the vicinity of lignite coal indicating that the CR biochar can be used as lignite coal. Therefore, to produce CR biochar with the promising fuel property under cost-advantage sweeping gas, torrefaction at 300 °C under 50 mL/min CO_2 was suggested. In comparison to other work, the atomic ratios of CR biochar from 300 °C torrefaction were higher than those of ground coffee residue (GCR) biochar, which located in the sub-bituminous area [31].

The influence of torrefaction on cassava rhizome (CR) was observed through the parameters of decarbonization (DC), dehydrogenation (DH), and deoxygenation (DO) as depicted in Fig. 5. DC, DH, and DO are used to define the decrease of mass of carbon, hydrogen, and oxygen in initial CR due to torefaction, respectively [18]. The percentages of DC, DH, and DO in this study increased remarkably with increasing process temperature from 200 to 300 °C. DC, DH, and DO of CR biochar from torrefaction under N_2 and mixture gas atmosphere were slightly higher than those under CO_2 atmosphere. On the other hand, an increase in CO_2 flow rate from 50 to 250 mL/min resulted DC, DH, and DO raised marginally from 30.25 to 32.27%, 53.45–54.66%, and 66.72–67.14%, respectively. The similar trends of these results were reported for torrefaction of microalga residue [18]. These results indicated that torrefaction has much higher effect on DO and DH than DC particularly at severe condition. It could therefore be ascribed that torrefaction affected dramatically oxygen and hydrogen contents in original CR. The changes in DO, DH, and DC levels are associated with the evaporation of volatile content and degradation of lignocellulosic compositions [5] over the dehydration, devolatilization, and decomposition reactions [32]. These corresponded to diminishing of H/C and O/C atomic ratios, and raising in biochar HHV. Furthermore, the varies

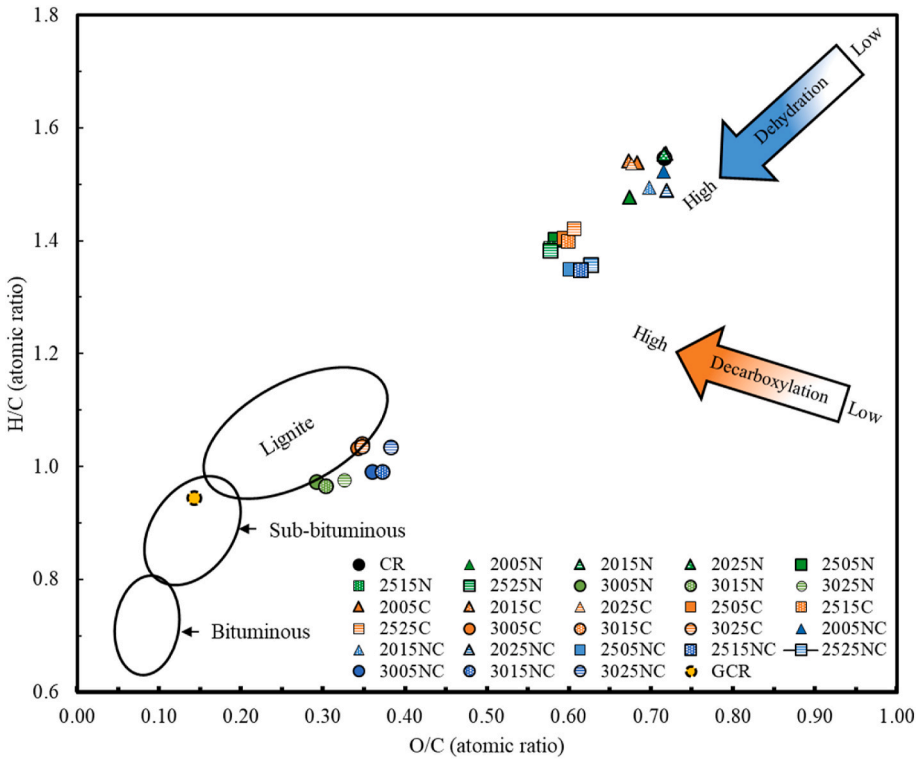

Fig. 4. Van-Krevelen diagram of CR and biochar from torrefaction of CR at different process conditions.

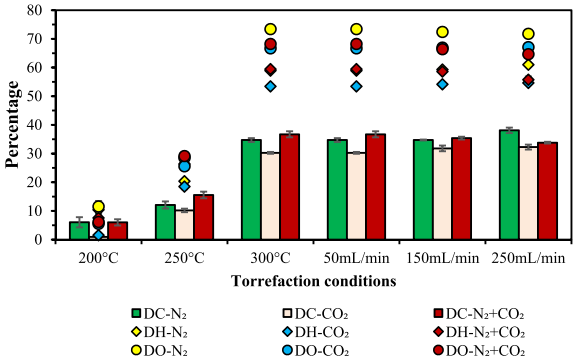

Fig. 5. Decarbonization (DC), dehydrogenation (DH), and deoxygenation (DO) of biochar from torrefaction of CR at different process conditions.

of DO, DH, and DC were regardless of sweeping gas type and flow rate. Also, these results confirmed that CO_2 can be used replacing N_2 in the production of solid fuel via torrefaction process.

3.3. Thermal stability characteristics

Thermal stability characteristics of cassava rhizome (CR) and the biochar from torrefaction at 300 °C for 30 min under different sweeping gas types (N_2, CO_2, and $N_2 + CO_2$) and flow rates (50, 150, 250 mL/min) are illustrated through thermogravimetry (TG) and derivative thermogravimetry (DTG) curves in Fig. 6(A) and (B), respectively. DTG curve shows that thermal degradation characteristics of original CR could be distinguished into three phases. The first phase was between 40 and 130 °C with one sharp peak at 75 °C. The presence of this phase is due to the vaporization of moisture content and volatile composition. The second phase started from 150 to 400 °C with the dominant peak present at 305 °C, and this was ascribed to the degradation of holocellulose (cellulose and hemicellulose) [33]. The last phase started from 410 to 600 °C which describes the degradation of lignin. Consistent findings on the degradation of holocellulose and lignin were presented in sugarcane bagasse [9], and corncob [34]. The holocellulose degradation was found to be in the range of 200–380 °C and 220–460 °C in sugarcane bagasse and corncob, respectively, whereas lignin degradation in sugarcane bagasse and corncob was found to be in the range of 440–540 °C, and 460–500 °C, respectively [5,9].

The thermal degradation characteristics of CR biochar were remarkably different from original CR. Table 2 demonstrates that the existing residue after thermal stability analysis of biochar was much higher than that of original CR (TG curve), the maximum mass loss rate (DTG_{max}) of original CR was substantially higher than that of CR biochar, and thermal degradation in second phase (T_{max} (°C)) of CR biochar was moved to higher temperature than that of original CR. This indicated that thermal stability of CR biochar was higher than that of original CR. On the other hand, the existing residue and mass loss rate were affected only marginally by sweeping gas type and flow rate. Therefore, the biochar with high thermal stability could be produced from torrefaction under 50 mL/min CO_2 atmosphere.

3.4. Chemical functional groups

Chemical functional groups of original cassava rhizome (CR) and biochar from torrefaction of CR at 300 °C for 30 min under 50 mL/min of CO_2, $CO_2 + N_2$, and N_2 are illustrated through FTIR spectra in Fig. 7. The spectra of CR were substantially different from that of biochar as there were some disappearing peaks due to chemical bond breakage during torrefaction. On the other hand, varying of sweeping gas types did not show a noticeable difference of the spectra indicating that CO_2 can be used as a sweeping gas in torrefaction

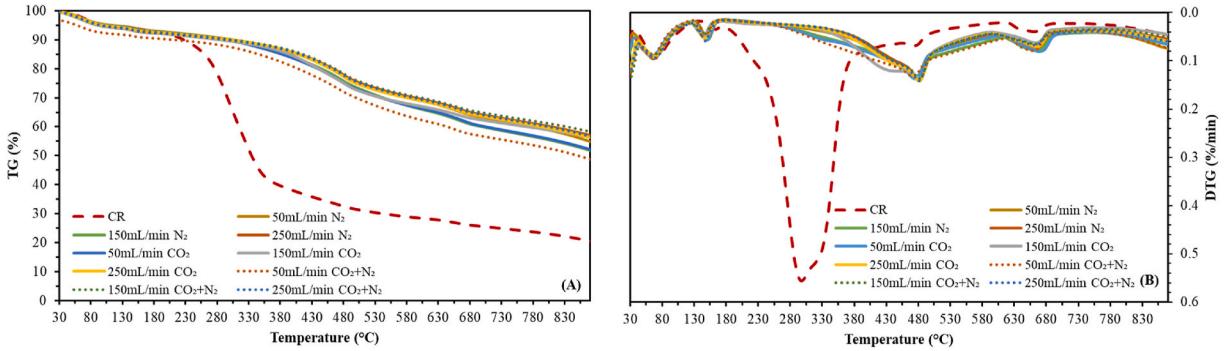

Fig. 6. TG (A) and DTG (B) curves of CR and biochar from torrefaction of CR under different atmospheric gas types and flow rates.

Table 2
Thermal stability parameters of initial CR and CR biochar.

Sample name	T_i (°C)	T_{max} (°C)	DTG_{max} (%/min)	Residue (%)
CR	71.45	298.15	0.55	19.80
50 mL/min N_2	153.05	477.23	0.13	53.78
150 mL/min N_2	149.33	478.84	0.13	50.77
250 mL/min N_2	145.89	480.60	0.14	56.22
50 mL/min CO_2	149.40	475.71	0.13	49.92
150 mL/min CO_2	145.87	482.40	0.14	55.62
250 mL/min CO_2	147.68	482.36	0.14	55.38
50 mL/min $CO_2 + N_2$	149.40	475.71	0.13	47.61
150 mL/min $CO_2 + N_2$	145.87	482.40	0.14	57.46
250 mL/min $CO_2 + N_2$	147.68	482.36	0.14	55.73

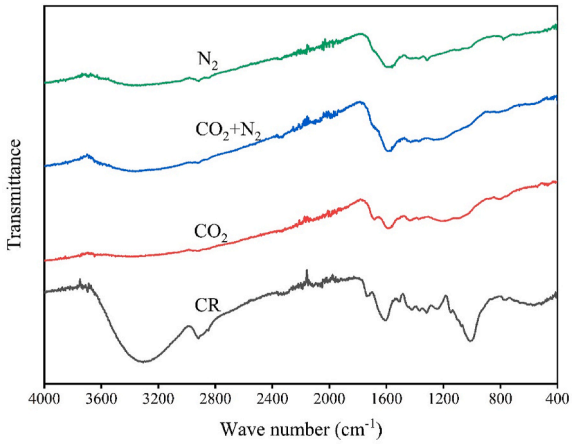

Fig. 7. FTIR spectra of CR and biochar from torrefaction of CR at different process conditions.

process. The signal peak presented at 3500-3300 cm^{-1} was assigned as the stretching vibration of hydroxyl (-OH) and carbonyl (C═O) groups [35]. It became less intense after torrefaction, indicating that dehydration reaction was taken place, which affected reducing of H/C and O/C atomic ratios, and enhancing DO, DH, and calorific content. In addition, the decrease of this peak intense determined that the hydrophobicity of biochar was improved. The peak at 2920-2850 cm^{-1} was attributed to C–H stretching vibration of aliphatic hydrocharbon [9]. The intensity of this peak dminished noticeably after torrefaction indicating that aliphatic hydrocarbon in CR could be damaged by torrefaction. The transmittance peak at 1650 cm^{-1} represented the C═O stretching vibration of ketone, amide, and carboxylic groups [36]. The decrease of this peak intense after torrefaction related to decarboxylation reaction. The bands at 1605 and 1510 cm^{-1} were ascribed to C═C stretching vibration of aromatic ring in lignin [36]. The existence of this peak after torrefaction indicated that lignin could not be totally degraded during torrefaction. The peak at 1050 cm^{-1} was due to stretching band of aliphatic ether C–O and alcohol C–O in cellulose and hemicellulose [36]. This disappeared after torrefaction implying that cellulose and hemicellulose were degraded possibly through decarboxylation reaction during torrefaction process.

3.5. Surface morphology

Surface morphology of biochar from torrefaction of cassava rhizome (CR) under different temperatures (200–300 °C) and atmospheric gas types (N_2, CO_2, and $N_2 + CO_2$) and flow rates (50, 150, 250 mL/min) are illustrated in Fig. 8. The original CR shows the smooth lamellar structure with flat surface. The surface was marginally destructed after torrefaction at 200 °C. An increase in process temperature caused it damaged noticeably, the cracks with groves and voids appeared on the surface. This change was mainly due to the devolatilization and depolymerization of the original CR, which corresponded with reducing of volatile and oxygen contents in elemental analysis results. On the other hand, the change of sweeping gas type or flow rate did not present a substantial effect on surface morphology.

3.6. Economic feasibility analysis

The diagram in Fig. 9 illustrates the economic analysis of CR torrefaction at 300 °C under 50 mL/min of carbon dioxide (CO_2) (Fig. 9A) and nitrogen (N_2) (Fig. 9B) atmospheres (see procedures in supplementary material for detailed calculation) [37,38]. The total input cost in torrefaction process under 50 mL/min CO_2 is composed of the cost of feedstock, labour, and energy (energy for chopping and pulverizing, drying, and torrefying) as tabulated in Table 3. Feedstock and labour cost were 20.00$/ton, and 20.00 $/5

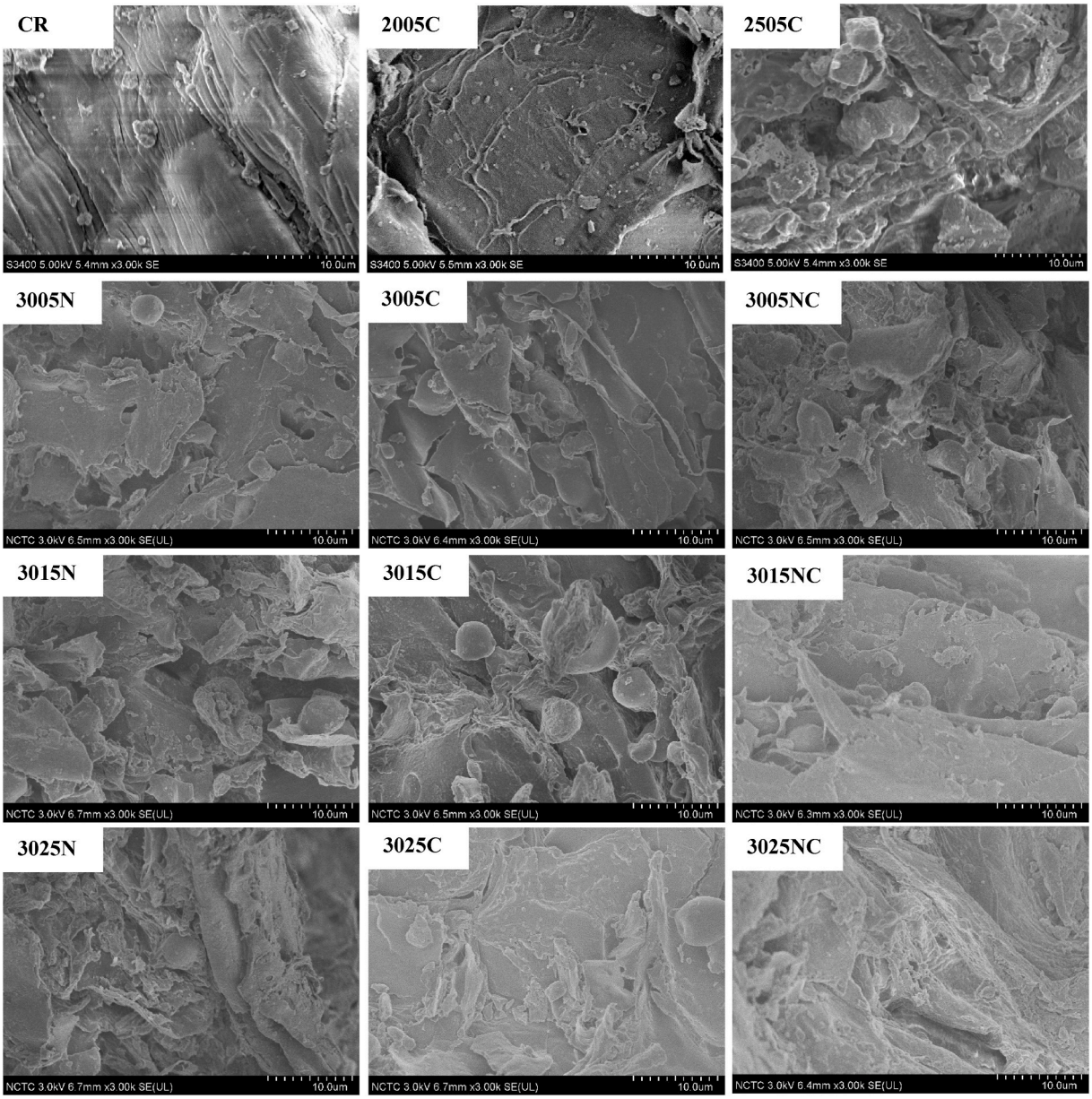

Fig. 8. Surface morphology of biochar from torrefaction of CR at different process conditions.

man-ton, respectively. During torrefaction of a ton of original CR, the energy for chopping and pulverizing, drying, and torrefying were 150.01, 1,986.02, and 444.65 MJ, respectively, which is equivalent to 716.85 kWh or 74.12 $ based on the electricity charge of 0.1 $/kWh. Thus, the total input cost of CR torrefaction at the proposed condition was 114.12 $/ton original CR. In comparison with the average cost of conventional char in Thailand in 2020 which was 515$/ton, thus it is equivalent to 140$ when calculated based on 1 ton of original CR. This implies that there is an initial profit of 140–114.12 or approximately 25.88$. In the case where N_2 was used as a sweep gas, there would be an additional cost of 25 $/ton original CR charged into the process [39], which means that there is an economical risk in this application. Hence, the use of CO_2 is considered a significant parameter for the actual use of such process. In addition, cost benefit output analysis based on the data of total operating cost and captical investment is tabulated in Table 3. The investment of torrefaction process is 4,800,647 $/ton original CR), it has the capacity of 2 tons raw CR/hr for operational time in 24 h/day and 250 day/year [40]. The analysis result determined that simple payback period of torrefaction process under 50 mL/min CO_2 is 15.46 years.

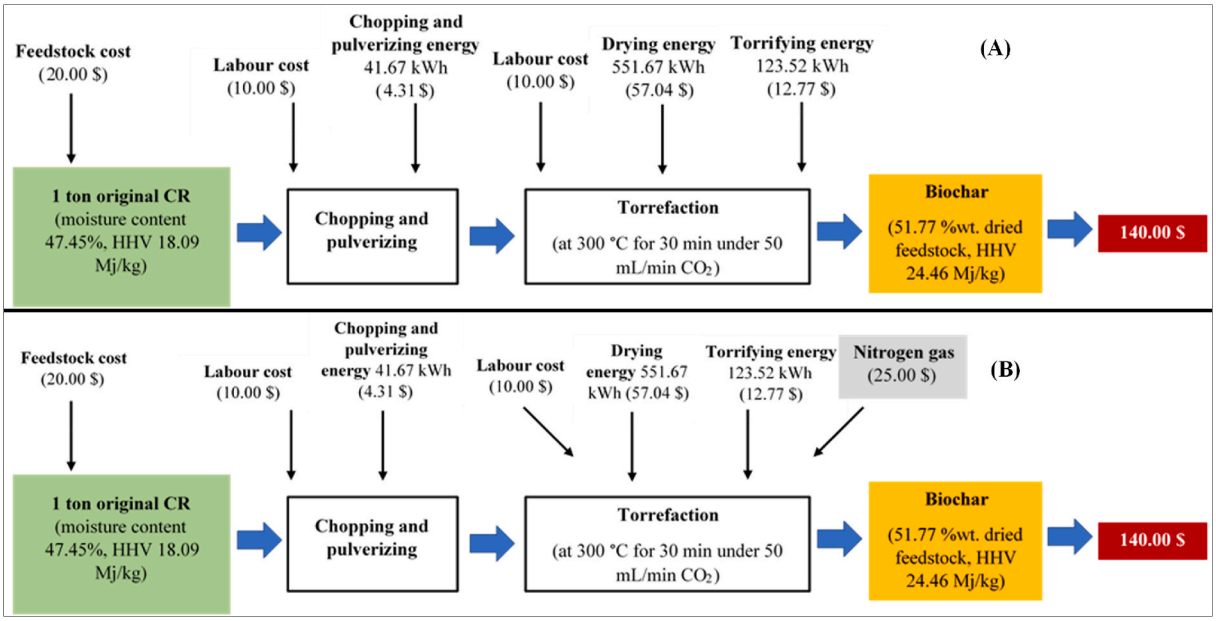

Fig. 9. Economic analysis of CR torrefaction under carbon dioxide (CO_2) atmosphere (A) and nitrogen (N_2) atmosphere (B).

Table 3
Economic analysis.

	1 ton original CR
1) Feedstock properties	
1.1) Mass (kg)	1,000.00
1.2) Moisture content (%)	47.45
1.3) Moist mass ($M_{mctb(L)}$;kg)	474.50
1.4) Dried feed mass ($M_{b(dry)}$; kg)	525.50
1.5) $ED_{b(dry)}$ (Mj/kg)	18.09
1.6) Cost ($/ton)	20.00
2) Choping and pulverizing energy	
2.1) Energy for choping and pulverizing (Mj/ton original CR) [38]	150.01
2.2) Electricity for choping and pulverizing (kWh/ton original CR)	41.67
2.3) Cost for choping and pulverizing ($/ton original CR)	4.31
3) Drying energy	
3.1) E_{mc} (Mj/kg)	0.31
3.2) Ed_{mc} (Mj/kg)	4.19
3.3) $Ed_{mc(net)}$ (Mj/ton original CR)	1,986.02
3.4) Drying electricity (kWh/ton original CR)	551.67
3.5) Drying cost ($/ton original CR)	57.04
4) Torrefying energy	
4.1) $E_{tb(dry)}$ (Mj/kg)	0.85
4.2) $E_{tb(net)(dry)}$ (Mj/ton original CR)	444.65
4.3) Torrefying electricity (kWh/ton original CR)	123.51
4.4) Torrying cost ($/ton original CR)	12.77
5) Labour cost	
5.1) Cost of 1 ton CR ($/4 man/ton original CR)	20.00
Total operating cost (Cost of feedstock, choping and pulverizing energy, drying energy, torrefying energy, and labour) ($/ton original CR)	**114.12**
6) Captical investment	
Torrefaction process with the capacity 2 tons raw CR/hr. (Operation of 24 h/day and 250 day/year) ($/ton original CR) [40]	4,800,647.00
7) Characteristics of the obtained biochar	
7.1) Yield (% wt. dried CR)	51.77
7.2) Yield (kg)	272.05
7.3) HHV (Mj/kg)	24.46
7.4) Total energy product (Mj/ton original CR)	6,654.38
7.5) Biochar price ($/ton original CR)	140.00
8) Cost benefit output analysis	
8.1) Simple payback period (Years)	15.46

4. Conclusions

In this study, CR was converted to biochar through torrefaction under nitrogen (N_2), carbon dioxide (CO_2), and gas mixtures (N_2 and CO_2 ratio 1:1) at different flowrates (50–250 mL/min), and process temperatures (200–300 °C) for 30 min. The experimental results are concluded that:

- CR can be converted to biochar as coal replacing material through 300 °C torrefaction under low CO_2 flow rate.
- Sweeping gas affected only slightly on fuel properties of biochar. Mass yield of CR biochar from severe torrefaction under N_2, CO_2, and gas mixtures was 47.39–50.21%, 51.44–52.81%, and 50.24–52.81%, respectively which its HHV of 23.97–24.54 Mj/kg, 23.70–24.46 Mj/kg, and 22.83–23.03 Mj/kg, respectively. Thus, it was concluded that CO_2 could readily be used to replace N_2 during torrefaction.
- The economic analysis emphasized the importance of using waste CO_2 as this rendered the process become economically feasible.

Declaration of competing interest

The authors declare that they have no known competing financial interests or personal relationships that could have appeared to influence the work reported in this paper.

Acknowledgements

This research project was supported by Mahidol University (Grant ID: A37/2561) and Nanomaterial for Energy and Catalyst Laboratory, National Nanotechnology Center (NANOTEC), National Science and Technology Development Agency (NSTDA). This study was partially supported for publication by the China Medical Board (CMB), Center of Excellence on Environmental Health and Toxicology (EHT), Faculty of Public Health, Mahidol University, Thailand.

Appendix A. Supplementary data

Supplementary data to this article can be found online at https://doi.org/10.1016/j.csite.2020.100823.

References

[1] W.-H. Chen, Chapter 10 - torrefaction, in: A. Pandey, S. Negi, P. Binod, C. Larroche (Eds.), Pretreatment of Biomass, Elsevier, Amsterdam, 2015, pp. 173–192, https://doi.org/10.1016/B978-0-12-800080-9.00010-4.
[2] P. Adams, T. Bridgwater, A. Lea-Langton, A. Ross, I. Watson, Chapter 8 - biomass conversion technologies, in: P. Thornley, P. Adams (Eds.), Greenhouse Gas Balances of Bioenergy Systems, Academic Press, 2018, pp. 107–139, https://doi.org/10.1016/B978-0-08-101036-5.00008-2.
[3] S. Gent, M. Twedt, C. Gerometta, E. Almberg, Chapter three - fundamental theories of torrefaction by thermochemical conversion, in: S. Gent, M. Twedt, C. Gerometta, E. Almberg (Eds.), Theoretical and Applied Aspects of Biomass Torrefaction, Butterworth-Heinemann, 2017, pp. 41–75, https://doi.org/10.1016/B978-0-12-809483-9.00003-8.
[4] J.M. Commandré, A. Leboeuf, Volatile yields and solid grindability after torrefaction of various biomass types, Environ. Prog. Sustain. Energy 34 (4) (2015) 1180–1186, https://doi.org/10.1002/ep.12073.
[5] S.-X. Li, C.-Z. Chen, M.-F. Li, X. Xiao, Torrefaction of corncob to produce charcoal under nitrogen and carbon dioxide atmospheres, Bioresour. Technol. 249 (2018) 348–353, https://doi.org/10.1016/j.biortech.2017.10.026.
[6] C. Couhert, S. Salvador, J.M. Commandré, Impact of torrefaction on syngas production from wood, Fuel 88 (11) (2009) 2286–2290, https://doi.org/10.1016/j.fuel.2009.05.003.
[7] L. Chai, C.M. Saffron, Comparing pelletization and torrefaction depots: optimization of depot capacity and biomass moisture to determine the minimum production cost, Appl. Energy 163 (2016) 387–395, https://doi.org/10.1016/j.apenergy.2015.11.018.
[8] Y.Y. Gan, H.C. Ong, T.C. Ling, W.-H. Chen, C.T. Chong, Torrefaction of de-oiled Jatropha seed kernel biomass for solid fuel production, Energy 170 (2019) 367–374, https://doi.org/10.1016/j.energy.2018.12.026.
[9] K. Manatura, Inert torrefaction of sugarcane bagasse to improve its fuel properties, Case Studies in Thermal Engineering 19 (2020) 100623, https://doi.org/10.1016/j.csite.2020.100623.
[10] O. Kutlu, G. Kocar, Upgrading lignocellulosic waste to fuel by torrefaction: characterisation and process optimization by response surface methodology, Int. J. Energy Res. 42 (15) (2018) 4746–4760, https://doi.org/10.1002/er.4228.
[11] Department of Agriculture, Agricultural Production Data, 2019. http://www.oae.go.th/assets/portals/1/fileups/prcaidata/files/casava%20dit%2062.pdf. (Accessed 30 May 2020).
[12] Department of Alternative Energy Development and Efficiency (DEDE), Biomass Potential in Thailand, 2013. http://weben.dede.go.th/webmax/content/biomass-database-potential-thailand. (Accessed 21 June 2020).
[13] A. Pattiya, J.O. Titiloye, A.V. Bridgwater, Fast pyrolysis of cassava rhizome in the presence of catalysts, J. Anal. Appl. Pyrol. 81 (1) (2008) 72–79, https://doi.org/10.1016/j.jaap.2007.09.002.
[14] K. Meesukanun, C. Satirapipathkul, Production of acetone-butanol-ethanol from cassava rhizome hydrolysate by Clostridium saccharobutylicum BAA 117, Chemical Engineering Transactions 37 (2014) 421–426, https://doi.org/10.3303/CET1437071.
[15] K. Nakason, B. Panyapinyopol, V. Kanokkantapong, N. Viriya-empikul, W. Kraithong, P. Pavasant, Characteristics of hydrochar and liquid fraction from hydrothermal carbonization of cassava rhizome, J. Energy Inst. 91 (2) (2018) 184–193, https://doi.org/10.1016/j.joei.2017.01.002.
[16] A. Sluiter, B. Hames, R. Ruiz, C. Scarlata, J. Sluiter, D. Templeton, Determination of ash in biomass (NREL/TP-510-42622), The US national renewable energy laboratory technical report (2008).
[17] ASTM, Standard Test Methods for Proximate Analysis of Coal and Coke by Macro Thermogravimetric Analysis, ASTM International, Pennsylvania, 2010. Method D7582-10.

[18] Y.-C. Chen, W.-H. Chen, B.-J. Lin, J.-S. Chang, H.C. Ong, Impact of torrefaction on the composition, structure and reactivity of a microalga residue, Appl. Energy 181 (2016) 110–119, https://doi.org/10.1016/j.apenergy.2016.07.130.
[19] Y. Uemura, W.N. Omar, T. Tsutsui, S.B. Yusup, Torrefaction of oil palm wastes, Fuel 90 (8) (2011) 2585–2591, https://doi.org/10.1016/j.fuel.2011.03.021.
[20] A. Zheng, Z. Zhao, S. Chang, Z. Huang, X. Wang, F. He, H. Li, Effect of torrefaction on structure and fast pyrolysis behavior of corncobs, Bioresour. Technol. 128 (2013) 370–377, https://doi.org/10.1016/j.biortech.2012.10.067.
[21] G. Pilon, J.-M. Lavoie, Pyrolysis of switchgrass (Panicum virgatum L.) at low temperatures within N_2 and CO_2 environments: product yield study, ACS Sustain. Chem. Eng. 1 (1) (2013) 198–204, https://doi.org/10.1021/sc300098e.
[22] W.-H. Chen, J. Peng, X.T. Bi, A state-of-the-art review of biomass torrefaction, densification and applications, Renew. Sustain. Energy Rev. 44 (2015) 847–866, https://doi.org/10.1016/j.rser.2014.12.039.
[23] W.-H. Chen, B.-J. Lin, B. Colin, J.-S. Chang, A. Pétrissans, X. Bi, M. Pétrissans, Hygroscopic transformation of woody biomass torrefaction for carbon storage, Appl. Energy 231 (2018) 768–776, https://doi.org/10.1016/j.apenergy.2018.09.135.
[24] A.B. Hernández, F. Okonta, N. Freeman, Sewage sludge charcoal production by N2- and CO2-torrefaction, Journal of Environmental Chemical Engineering 5 (5) (2017) 4406–4414, https://doi.org/10.1016/j.jece.2017.08.001.
[25] D. Kim, K. Lee, K.Y. Park, Upgrading the characteristics of biochar from cellulose, lignin, and xylan for solid biofuel production from biomass by hydrothermal carbonization, J. Ind. Eng. Chem. 42 (2016) 95–100, https://doi.org/10.1016/j.jiec.2016.07.037.
[26] J. Kongpanya, K. Hussaro, S. Teekasap, Influence of reaction temperature and reaction time on product from hydrothermal treatment of biomass residue, Am. J. Environ. Sci. 10 (4) (2014) 324–335, https://doi.org/10.3844/ajessp.2014.324.335.
[27] M. Asadullah, A.M. Adi, N. Suhada, N.H. Malek, M.I. Saringat, A. Azdarpour, Optimization of palm kernel shell torrefaction to produce energy densified bio-coal, Energy Convers. Manag. 88 (2014) 1086–1093, https://doi.org/10.1016/j.enconman.2014.04.071.
[28] M.T. Reza, B. Wirth, U. Lüder, M. Werner, Behavior of selected hydrolyzed and dehydrated products during hydrothermal carbonization of biomass, Bioresour. Technol. 169 (2014) 352–361, https://doi.org/10.1016/j.biortech.2014.07.010.
[29] Z. Liu, A. Quek, S. Kent Hoekman, R. Balasubramanian, Production of solid biochar fuel from waste biomass by hydrothermal carbonization, Fuel 103 (2013) 943–949, https://doi.org/10.1016/j.fuel.2012.07.069.
[30] M. Beychok, Coal, 2012. http://www.eoearth.org/view/article/151276. (Accessed 30 May 2020).
[31] J. Pathomrotsakun, K. Nakason, W. Kraithong, P. Khemthong, B. Panyapinyopol, P. Pavasant, Fuel properties of biochar from torrefaction of ground coffee residue: effect of process temperature, time, and sweeping gas, Biomass Conversion and Biorefinery 10 (3) (2020) 743–753, https://doi.org/10.1007/s13399-020-00632-1.
[32] C. Zhang, S.-H. Ho, W.-H. Chen, Y. Xie, Z. Liu, J.-S. Chang, Torrefaction performance and energy usage of biomass wastes and their correlations with torrefaction severity index, Appl. Energy 220 (2018) 598–604, https://doi.org/10.1016/j.apenergy.2018.03.129.
[33] S. Xin, T. Mi, X. Liu, F. Huang, Effect of torrefaction on the pyrolysis characteristics of high moisture herbaceous residues, Energy 152 (2018) 586–593, https://doi.org/10.1016/j.energy.2018.03.104.
[34] X. Tian, L. Dai, Y. Wang, Z. Zeng, S. Zhang, L. Jiang, X. Yang, L. Yue, Y. Liu, R. Ruan, Influence of torrefaction pretreatment on corncobs: a study on fundamental characteristics, thermal behavior, and kinetic, Bioresour. Technol. 297 (2020) 122490, https://doi.org/10.1016/j.biortech.2019.122490.
[35] K.-T. Wu, C.-J. Tsai, C.-S. Chen, H.-W. Chen, The characteristics of torrefied microalgae, Appl. Energy 100 (2012) 52–57, https://doi.org/10.1016/j.apenergy.2012.03.002.
[36] N.D. Duranay, G. Akkuş, Solid fuel production with torrefaction from vineyard pruning waste, Biomass Conversion and Biorefinery (2019), https://doi.org/10.1007/s13399-019-00496-0.
[37] D. Maski, M.J. Darr, R.P. Anex, Torrefaction of cellulosic biomass upgrading—energy and cost model, in: Agricultural and Biosystems Engineering Conference Proceedings and Presentations, American Society of Agricultural and Biological Engineers, Pittsburgh, PA, 2010, 2010.
[38] G.T. Douglas, L. Won Fy, M. Vance, K. Nalladurai, Economic analysis of biomass torrefaction plants integrated with corn ethanol plants and coal-fired power plants, Advances in Energy Research 1 (2) (2013) 127–146, https://doi.org/10.12989/eri.2013.1.2.127.
[39] F. Mike, Air best practices, The Energy Costs Associated with Nitrogen Specifications, 2020. https://www.airbestpractices.com/system-assessments/air-treatmentn2/energy-costs-associated-nitrogen-specifications. (Accessed 21 June 2020).
[40] Australian Meat Processor Corporation (AMPC), Review and Cost Benefit Analysis of Torrefaction Technology for Processing Abattoir Waste, 2015, in: https://www.ampc.com.au/2015/01/Review-cost-benefit-analysis-of-Torrefaction-technology-for-processing-abattoir-waste-Review-and-cost-benefit-analysis-of-Torrefaction-technology-for-processing-abattoir-waste. (Accessed 20 June 2020).